Science of the Total Environment 593–594 (2017) 462–469

Contents lists available at ScienceDirect

Science of the Total Environment

journal homepage: www.elsevier.com/locate/scitotenv

Primary particulate emissions and secondary organic aerosol (SOA) formation from idling diesel vehicle exhaust in China

DengWei [a,c], HuQihou [a], LiuTengyu [a], WangXinming [a,b,*], ZhangYanli [a,b], SongWei [a], SunYele [d], BiXinhui [a], YuJianzhen [e], YangWeiqiang [a,c], HuangXinyu [a,c], ZhangZhou [a], HuangZhonghui [a,c], HeQuanfu [a], Abdelwahid Mellouki [f], Christian George [g]

[a] State Key Laboratory of Organic Geochemistry and Guangdong Key Laboratory of Environmental Protection and Resources Utilization, Guangzhou Institute of Geochemistry, Chinese Academy of Sciences, Guangzhou 510640, China
[b] Center for Excellence in Regional Atmospheric Environment, Institute of Urban Environment, Chinese Academy of Sciences, Xiamen 361021, China
[c] University of Chinese Academy of Sciences, Beijing 100049, China
[d] Institute of Atmospheric Physics, Chinese Academy of Sciences, Beijing 100029, China
[e] Division of Environment, Hong Kong University of Science & Technology, Clear Water Bay, Kowloon, Hong Kong, China
[f] Institut de Combustion, Aérothermique, Réactivité et Environnement (ICARE), CNRS, 45071 Orléans Cedex 02, France
[g] Institut de Recherches sur la Catalyse et l'Environnement de Lyon (IRCELYON), CNRS, UMR5256, Villeurbanne F-69626, France

HIGHLIGHTS

- Primary and secondary OA of diesel exhaust characterized with a smog chamber.
- Much higher primary and secondary OA from diesel vehicles than gasoline ones
- Higher diesel vehicle primary emission and secondary production of OA in China
- Traditional precursor VOCs explained less than 3% SOA formed during aging.
- Particle number emission factors of $0.65–4.0 \times 10^{15}$ # kg-fuel^{-1} for diesel vehicles

GRAPHICAL ABSTRACT

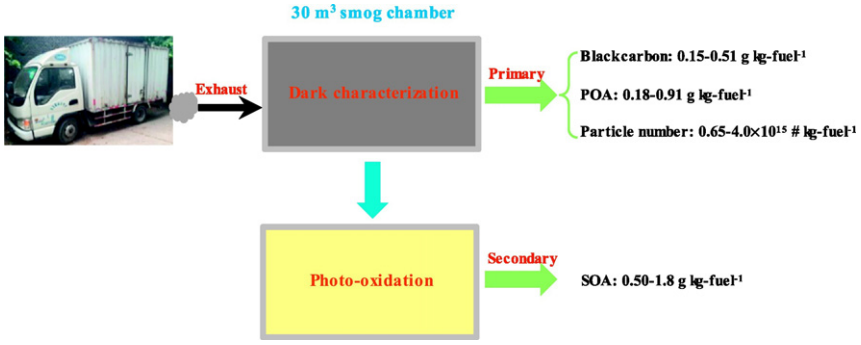

ARTICLE INFO

Article history:
Received 6 February 2017
Received in revised form 8 March 2017
Accepted 9 March 2017
Available online 27 March 2017

Editor: D. Barcelo

Keywords:
Diesel vehicles
Primary organic aerosols
Secondary organic aerosols
Black carbon
Particle number
Chamber simulation

ABSTRACT

In China diesel vehicles dominate the primary emission of particulate matters from on-road vehicles, and they might also contribute substantially to the formation of secondary organic aerosols (SOA). In this study tailpipe exhaust of three typical in-use diesel vehicles under warm idling conditions was introduced directly into an indoor smog chamber with a 30 m^3 Teflon reactor to characterize primary emissions and SOA formation during photo-oxidation. The emission factors of primary organic aerosol (POA) and black carbon (BC) for the three types of Chinese diesel vehicles ranged 0.18–0.91 and 0.15–0.51 g kg-fuel^{-1}, respectively; and the SOA production factors ranged 0.50–1.8 g kg-fuel^{-1} and SOA/POA ratios ranged 0.7–3.7 with an average of 2.2. The fuel-based POA emission factors and SOA production factors from this study for idling diesel vehicle exhaust were 1–3 orders of magnitude higher than those reported in previous studies for idling gasoline vehicle exhaust. The emission factors for total particle numbers were $0.65–4.0 \times 10^{15}$ particles kg-fuel^{-1}, and particles with diameters less than 50 nm dominated in total particle numbers. Traditional C_2-C_{12} precursor non-methane hydrocarbons (NMHCs) could only explain less than 3% of the SOA formed during aging and contribution from other precursors including intermediate volatile organic compounds (IVOC) needs further investigation.

* Corresponding author at: State Key Laboratory of Organic Geochemistry, Guangzhou Institute of Geochemistry, Chinese Academy of Sciences, China.
E-mail address: wangxm@gig.ac.cn (X. Wang).

http://dx.doi.org/10.1016/j.scitotenv.2017.03.088
0048-9697/

1. Introduction

Particulate matter (PM) with aerodynamic diameter less than 2.5 μm ($PM_{2.5}$) has attracted an increasing concern in densely populated megacities, such as China's capital city Beijing (Guo et al., 2014; Huang et al., 2014), due to its adversely effects on human health by causing respiratory and cardiopulmonary diseases (Pope et al., 2009; Brook et al., 2010; Liu et al., 2015b;Lelieveld et al., 2015). In urban agglomerations, vehicle exhaust contributes substantially to $PM_{2.5}$, with mass fractions ranging from ~22% in southeastern US (Chen et al., 2012), ~37% in Guangzhou in the Pearl River Delta during wet season (Cui et al., 2015), to as high as 49% in Mexico City (Stone et al., 2008). In particular, people are usually exposed to much more serious air pollution in urban roadside microenvironments due to traffic-related emissions (Zhao et al., 2004; Xu et al., 2008). Therefore, vehicle emissions could pose serious health concern and deserve intensive investigation.

Direct motor vehicle emission of PM is predominantly from diesel vehicles (Reff et al., 2009; Zhang et al., 2009). In China diesel vehicles contributed more than 99% of primary vehicle emission of PM, although they only account for 15.2% of China's on-road vehicles (MEPC, 2014). Recent studies revealed that diesel vehicles could contribute 80%–90% of PM emissions from on-road sources in Chinese cities (Huo et al., 2011; Wu et al., 2010; Wang et al., 2010). Hence, quite a few studies had put their focus on characterizing primary diesel vehicle emissions in the last decade, either through tunnel tests (Huang et al., 2006; Zhang et al., 2016), or, in particular using a portable emissions measurement system (PEMS) to test on-road emission of air pollutants such as PM, VOCs and black carbon (Liu et al., 2009; Wu et al., 2015; Yao et al., 2015; Zheng et al., 2015; Wu et al., 2016). While these studies have greatly enriched our knowledge about primary emissions from diesel vehicles in China, the contribution of diesel vehicle exhaust to secondary products formed through photo-oxidation, however, still remains unknown.

Diesel vehicle exhaust also contributes substantially to secondary organic and inorganic aerosols *via* photo-oxidation of primary emissions, such as intermediate volatile organic compounds (IVOCs) and nitrogen oxides (NO_x) (Weitkamp et al., 2007; Robinson et al., 2007; Samy and Zielinska, 2010; Nakao et al., 2011; Zhao et al., 2015). Unlike gasoline vehicle exhaust, diesel-related IVOCs could be a dominant local source of SOA (Dunmore et al., 2015; Ots et al., 2016). Robinson et al. (2007) reported substantial SOA formation from photo-oxidization of a diluted diesel engine exhaust for the first time. Chirico et al. (2010) investigated SOA formation from 3 in-use diesel vehicles in Europe. Gordon et al. (2014b) simulated SOA production from 5 diesel vehicles in the US. However, there is no chamber simulation study available on the SOA formation from China diesel vehicle exhausts, and it is not clear whether SOA formation from diesel vehicle exhaust in China resembles that in USA or Europe. Vehicle emission characteristics depend strongly on fuel quality, vehicle technologies, and operating conditions (Rogge et al., 1993; Miracolo et al., 2012; Cross et al., 2015). As diesel vehicles in China are equipped with engines that are mainly designed and produced domestically with technology lagging behind developed nations, and the diesel fuel quality in China and the developed nations also differs markedly (Wang et al., 2015), consequently the emission of PM, NO_x, SO_2, NH_3 and hydrocarbons (HC) from diesel vehicles in China might be different from that in the developed nations (Liu et al., 2014; Zhang et al., 2015). Therefore, there might be differences in SOA formation from China diesel vehicle exhaust, and it is necessary to investigate the SOA formation from diesel vehicle exhaust in China to provide valuable information for making effective control policies to alleviate the serious PM air pollution.

In this study, we chose three typical types of diesel vehicles made in China, introduced the exhaust from the diesel vehicles under warm idling conditions into an indoor smog chamber with a 30 m^3 reactor, and investigated the primary emissions and SOA formation under photo-oxidation. The main purpose of this study is to obtain a more comprehensive evaluation of diesel vehicle's contribution to carbonaceous aerosols.

2. Materials and methods

2.1. Vehicles and fuel

Table 1 lists the three diesel vehicles used for our chamber experiments. They represent three different types of diesel vehicles manufactured by three major diesel vehicle makers in China. Foton is a medium-duty passenger car made by the Baic Motor Corporation Ltd., Changan is a medium-duty truck made by the China Changan Automobile Group, and JAC is a heavy-duty truck made by JAC Motors. In 2011, annual production of diesel vehicles by the three companies were 490,280, 299,506 and 230,452, respectively (CAAM, 2011), and their diesel vehicle sales were all among the top 10 in China. All the vehicles in this study had no exhaust aftertreatment devices and they were fueled with Grade 0# diesel, which complies with the Euro III diesel fuel standard.

2.2. Experimental setup

The experiments were carried out in the indoor smog chamber at Guangzhou Institute of Geochemistry, Chinese Academy of Sciences (GIG-CAS). Details of setup and facilities about the chamber are described elsewhere (Wang et al., 2014; Liu et al., 2015a). Briefly, 135 black lamps (1.2 m long, 60 W Philips/10R BL, Royal Dutch Philips Electronics Ltd., the Netherlands) are used as a light source, providing a NO_2 photolysis rate of 0.25 min^{-1}. Temperature was set to 25 °C with an accuracy of ± 1 °C. The relative humidity (RH) was set to less than 5% (Table 2). Prior to each experiment, the Teflon chamber was flushed with dry purified air for at least 5 whole exchanges of the reactor volume to make sure it was clean.

Before introducing exhaust into the chamber reactor, the tested vehicle was started and run on-road for about 30 min before remaining at idling condition. Diesel vehicle exhaust was then introduced into the purified air filled chamber using a Dekati® ejector dilutor (DI-1000, Dekati Ltd., Finland) connected to the end of a stainless steel transfer line (0.5 in. i.d. and 15 m in length) heated at 100 °C. When the particle mass reached approximate 50 μg m^{-3}, which is comparable to the annual average value of $PM_{2.5}$ in Guangzhou in 2014 (Guangzhou Environmental Protection Bureau, 2015), exhaust injection was stopped. The injection time ranged from 5 to 20 min. The dilution ratios were estimated by measuring the CO_2 concentrations and are shown in Table 2.

After introducing exhaust, nitrous acid (HONO) was bubbled into the chamber as a source of hydroxyl radical (OH). Propene has often been added to adjust VOC/NO_x ratio in diesel exhaust chamber experiments (Chirico et al., 2010; Presto et al., 2014; Gordon et al., 2014b) and is not considered to be a relevant SOA precursor (Odum et al., 1996; Cocker et al., 2001). Here propene was also added to adjust the VOC/NO_x ratios to approximately 3:1 ppbC:ppb, which is considered a typical ratio for urban environments (Guo et al., 2013). 60 ppbv of deuterated butanol (butanol-d9) was also injected into the chamber as an OH tracer by using $k_{\text{butanol-d9}} = 3.4 \times 10{-}^{12}$ cm^3 $molecule^{-1}$ s^{-1} (Barmet et al., 2012; Gordon et al., 2014a). After characterizing the primary emission in dark conditions for an hour, the exhaust was photo-oxidized for 5 h through exposure to black lights.

2.3. Instrumentation

An array of instruments was used to monitor trace gases and particles inside the chamber. Ozone (O_3) was measured with an ozone analyzer (EC9810, Ecotech, Australia) and NO_x were measured with a trace nitrogen oxides analyzer (EC9841, Ecotech, Australia). SO_2 was measured with a dedicated analyzer (Model 43i, Thermo Scientific, USA).

Table 1
Information for the three diesel vehicles used in the experiments.

Vehicle ID	Vehicle type	Emission standard	Model year	Mileage (km)	Displacement (cm^{-3})	Power (kW)	Weight (kg)	Compression ratio
Foton	MDDV	Euro III	2011	16,000	2499	65	2580	17.4:1
Changan	MDDV	Euro III	2013	15,000	2540	67	3775	17.4:1
JAC	HDDV	Euro III	2013	11,000	9839	215	24,900	17.5:1

VOCs were measured online with a commercial proton-transfer-reaction time-of-flight mass spectrometer (PTR-ToF-MS, Model 2000, Ionicon Analytik GmbH, Austria) (Lindinger et al., 1998; Jordan et al., 2009). The concentrations of hydroxyl radical (OH) during the experiments were inferred from the decay of deuterated butanol measured with the PTR-ToF-MS (Atkinson and Arey, 2003). The average OH levels during our experiments were calculated to be approximate 2–5 × 10^6 molecules cm^{-3}, which is comparable to the levels in both ambient air and that in the previous study by Gordon et al. (2014b). Offline VOC samples were also collected using 2 L stainless steel canisters every 30 min during photo-oxidation, and measured by a Model 7100 Preconcentrator (Entech Instruments Inc., California, USA) coupled with an Agilent 5973 N gas chromatography-mass selective detector/flame ionization detector (GC-MSD/FID, Agilent Technologies, USA). CO in the canister samples was analyzed using a gas chromatography (6980GC, Agilent, USA) with a flame ionization detector and a packed column (5A molecular sieve 60/80 mesh, 3 m × 1/8 in.). Detailed procedures for the offline analysis of VOCs and CO are described elsewhere (Zhang et al., 2012). Before and after introducing exhaust, air samples were collected into 3 L cleaned Teflon bags to determine CO_2 concentrations with an HP 4890D gas chromatography (Yi et al., 2007).

A scanning mobility particle sizer (SMPS, Model 3080 classifier, model 3775 CPC; TSI Inc., Minnesota, USA) was used to measure the number and volume concentrations and size distributions of particles within 14–700 nm. The particle mass concentration was estimated assuming spherical particles and a density of 1.0 g cm^{-3} (Weitkamp et al., 2007). BC concentrations were measured with a seven-channel Aethalometer (Model AE-31, Magee Scientific, Berkeley, California). The Aethalometer data were corrected for particle loading effects using the method of Kirchstetter and Novakov (2007). A high-resolution time-of-flight aerosol mass spectrometer (HR-ToF-AMS, Aerodyne Research Inc., USA) operated in alternating V and W mode was used to measure non-refractory submicron aerosol mass and chemical compositions (Jayne et al., 2000; DeCarlo et al., 2006). The contribution of gas phase CO_2 to the AMS *m/z* 44 signal was corrected by analyzing HEPA filtered air from the smog chamber after filling the exhaust.

2.4. Operation steps

As shown in Fig. 1, each experiment consisted of five steps: 1) introducing exhaust into the chamber from $t = -2.3$ h. With the injection of exhaust, concentrations of NO_x, BC and OA were climbing. Their concentrations when the injection was stopped are given in Table 2. The mixing ratio of NO_x increased from 0 to ~1 ppmv; the particle number concentration increased rapidly from ~2 to ~350,000 particles cm^{-3}; the total particle mass concentrations increased from ~0 to over 100 μg m^{-3}; and the VOC concentrations also slightly increased at this step. 2) characterizing primary emissions from $t = -2$ h. After the injection, the increase of NO_x, BC, OA and VOCs were measured against that of CO_2 and CO, and the emission factors were further calculated. 3) adding HONO and propene at approximately $t = -0.2$ h, leading to a moderate increase in both NO and NO_2, approximately 300 ppbv for each. 4) turning on the lights at $t = 0$ h to start the photo-oxidation. Substantial amounts of SOA formed at the beginning of this period. 5) turning off the lights at $t = 5$ h and further characterizing the aged diesel vehicle exhaust in the dark for about 2 h.

2.5. Data analysis

The emission factors (EF) for various pollutants and the production factors (PF) for SOA were calculated on a fuel basis (g kg-$fuel^{-1}$):

$$EF_P \text{ or } PF_P = 10^3 \cdot [\Delta P] / \left(\frac{[\Delta CO_2]}{MW_{CO_2}} + \frac{[\Delta CO]}{MW_{CO}} \right) \cdot \frac{C_f}{MW_C} \quad (1)$$

and the emission factors of total particle number (EF_{TN}, # kg-$fuel^{-1}$) were calculated as follow:

$$EF_{TN} = 10^{15} \cdot [PN_{tot}] / \left(\frac{[\Delta CO_2]}{MW_{CO_2}} + \frac{[\Delta CO]}{MW_{CO}} \right) \cdot \frac{C_f}{MW_C} \quad (2)$$

where [△P] is the background corrected pollutant concentration in μg m^{-3}, PN_{tot} represents the total particle number concentration in # cm^{-3}. [△CO_2] and [△CO] are the background-subtracted concentration of CO_2 and CO in the chamber in μg m^{-3}. MW_{CO2}, MW_{CO} and MW_C are the molecular weights of CO_2 (44.1 g mol^{-1}), CO (28 g mol^{-1}) and carbon (12 g mol^{-1}), respectively. C_f is the mass fraction of carbon in the diesel fuel, which was adopted as 0.87 kg C kg-$fuel^{-1}$ for diesel (Chirico et al., 2010). Eq. (1) assumes that all carbon in the fuel was converted to CO_2 and CO, and the contribution from VOCs was negligible. This assumption is reasonable, because [△CO_2] and [△CO] after exhaust introduction were approximate 100 ppmv and 1 ppmv, respectively, while the increase of VOC was below 5 ppbv.

The loss of particles and condensable organic vapors onto the reactor walls need to be corrected to accurately quantify particle concentrations in the smog chamber. In this study, the AMS and SMPS data were corrected for wall loss using the method of Gordon et al. (2014b).

Table 2
Summary of the results for the chamber study experiments on diesel vehicle exhaust.

Expt. no.	Vehicle	T (°C)	RH (%)	NO[a] (ppbv)	NO_2[a] (ppbv)	Dilution ratio	OH (×10^6 molecules cm^{-3})	EF_{BC} (g kg^{-1} fuel)	EF_{POA} (g kg^{-1} fuel)	PF_{SOA} (g kg^{-1} fuel)	
										ω = 0	ω = 1
1	JAC	24.2	2.3	3246	220	71	3.11	0.16	0.19	0.30	0.61
2	Foton	24.9	2.5	1156	144	136	1.74	0.19	0.34	0.26	0.56
3	Foton	24.1	1.5	1185	136	115	5.23	0.18	0.28	0.28	0.68
4	Foton	24.9	2.7	749	153	213	5.00	0.19	0.32	0.34	0.76
5	Foton	25.2	2.4	2151	236	66	2.24	0.15	0.18	0.23	0.60
6	Changan	24.7	2.5	733	248	210	3.99	0.47	0.91	0.62	1.8
7	Changan	24.5	1.7	1113	43	214	4.23	0.50	0.74	0.39	0.50
8	Changan	24.6	2.3	1286	205	188	4.10	0.51	0.72	0.57	1.1

[a] Before adding HONO.

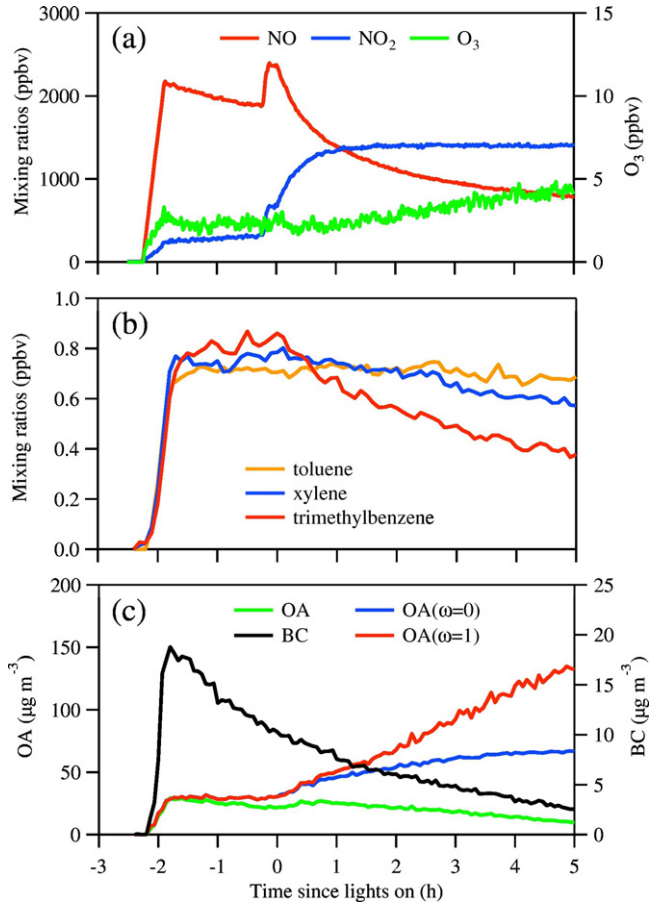

Fig. 1. Evolution of gaseous and particulate species during a typical smog chamber experiment (Experiment 4). Concentrations of (a) NO_x, O_3, (b) single-ring aromatic SOA precursors, and (c) measured OA and BC and wall loss corrected organic aerosol (OA(ω = 0) and OA(ω = 1)). $t = 0$ represents the time we turned on the black lights.

Briefly, particulate losses were quantified by assuming that the aerosol was internally mixed and thus, organic aerosol (OA) had the same wall-loss rates with BC. Two limiting cases were considered: ω = 0, no organic vapors condense to wall-bound particles; ω = 1, organic vapors remain in equilibrium with both wall-bound and suspended particles, where ω is a proportionality factor of organic vapor partitioning to chamber walls and suspended particles (Weitkamp et al., 2007).

For ω = 0, the loss rate of OA to the chamber walls is

$$\frac{d}{dt}(OA_{wall}) = -k \cdot OA_{sus} \tag{3}$$

where OA_{wall} and OA_{sus} are the wall-bounded and the suspended OA measured at time t, respectively, and k is the wall loss rate constant of BC. The total concentration of OA at time t ($OA_{total,t}$) was calculated by:

$$OA_{total,t} = OA_{sus}(t) + \int_0^t k \cdot OA_{sus}(t)dt \tag{4}$$

For ω = 1, the total concentration of OA at time t ($OA_{total,t}$) was estimated as:

$$OA_{total,t} = OA_{sus}(t) \times [BC(t_0)/BC(t)] \tag{5}$$

where $BC(t_0)$ is the initial BC concentration measured before lights are switched on and $BC(t)$ is the BC concentration after lights are turned on for a time span t.

In the experiments with low BC concentrations and significant SOA formation, the newly formed SOA was coated on preexisting particles, and then could enhance the BC mass absorption efficiency and artificially increase the estimated BC concentration (Schnaiter et al., 2005; Shiraiwa et al., 2010). Therefore, we corrected the wall loss effect using an exponential fit to the BC data rather than the actual BC data themselves (Gordon et al., 2014b):

$$OA_{total,t} = OA_{sus}(t)/e^{-kt} \tag{6}$$

where k is the wall loss rate constant of black carbon.

3. Results and discussions

3.1. Primary emission of particulate matters

The emission factors of POA and BC are displayed in Fig. 2. The EF_{BC} were 0.15–0.51 g kg-fuel^{-1} in this study, similar to that of 0.466–0.763 g kg-fuel^{-1} reported by Chirico et al. (2010) and ~0.260 g kg-fuel^{-1} by Gordon et al. (2014b) in chamber studies for exhaust from idling diesel vehicles. They were also comparable to that of 612 ± 740 mg kg fuel^{-1}, which were the emission factors of Euro III on-road diesel vehicle measured by using PEMS (Zheng et al., 2015). The EF_{POA} (0.18–0.91 g kg-fuel^{-1}) were higher than those reported in previous studies. For instance, the highest emission factors for POA reported by Chirico et al. (2010) were only 0.147 g kg-fuel^{-1}. Differences in diesel fuel compositions might be among the reasons the higher EFs of POA for China's diesel vehicles in this study. Lange et al. (1993) found that PM emissions could increase 15% when changing polyaromatic content of diesel fuel from 3.3 to 5.7%. Mi et al. (2000) revealed that the total polycyclic aromatic hydrocarbon (PAH) emission could increase 2.6 and 5.7 times and Fluorene emission would increase 52.9 and 152 times by adding 3% and 5% of Fluorene. As reported by Yue et al. (2015), the averaged content of PAHs in China III diesel is around 9% with a range of 2–18%, much higher than that in the fuel from Europe and the US. In diesel engine carbonaceous soot is formed in the center of spray where the air/fuel ratio is low (Yanowitz et al., 2000). As the soot cools, organic compounds derived from the fuel and the lubricating

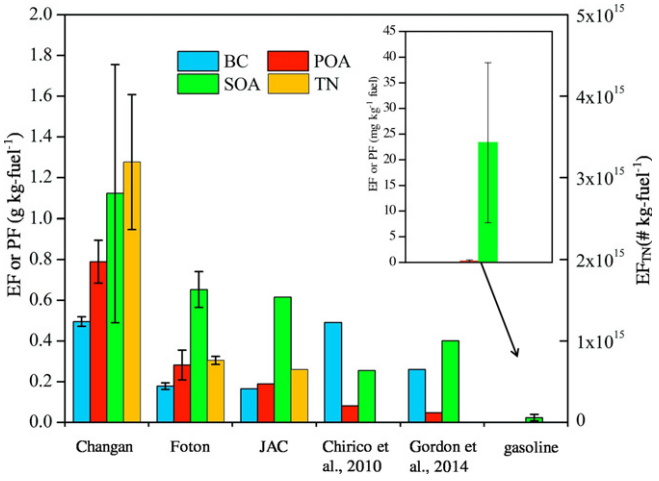

Fig. 2. Emission factors of BC, POA and production factors of SOA for ω = 1 (left axis) and emission factor of total particle number concentration (right axis) from different diesel vehicle exhausts in this study, as well as those from diesel and gasoline vehicle reported in the literature. The error bars represent the ranges of EFs and PFs for each vehicle. The emission factor reported by Chirico et al. (2010) is under idling condition for a MDDV without aftertreatment. The emission factor reported by Gordon et al. (2014b) is the result under creep + idling condition for a HDDV without aftertreatment. The emission factor for gasoline vehicle is from the dataset of Liu et al. (2015a), and BC is not reported but comparatively negligible. The right-hand side of the figure shows average values from 5 gasoline vehicle experiments from Liu et al. (2015a).

oil can be adsorbed onto the soot particles or form organic aerosol by nucleation (Abdul-Khalek et al., 1999; Yanowitz et al., 2000). Therefore higher content of semi-volatile PAHs in diesel could lead to more PAHs adsorb on soot particle and enhance the formation of POA.

The POA emission factor decreased with increasing dilution because of the evaporation of semi-volatile organic compounds (Lipsky and Robinson, 2006; Shrivastava et al., 2006; Robinson et al., 2007). This decrease can be well explained by the partitioning theory (Donahue et al., 2006; Shrivastava et al., 2006; Robinson et al., 2007). The partitioning theory described by Donahue et al. (2006) was used to estimate POA concentration in this study and check if dilution is reason for higher POA emission factors than those reported by Chirico et al. (2010) and Gordon et al. (2014b). Briefly, the fraction of compound *i* found in the condensed phase (ξ_i) was calculated as follow:

$$\xi_i = \left(1 + \frac{C_i^*}{C_{OA}}\right)^{-1} \quad (7)$$

where C_i^* is effective saturation concentrations. The following volatility basis set was used: $\{C_i^*\} = \{0.1, 1, 10, 100, 1000, 10{,}000, 100{,}000, 1000\,000\}$. C_{OA} represents the total mass concentration of organic aerosol. Therefore, the estimated OA concentration ($C_{Modeled}$) can be defined as:

$$C_{Modeled} = \sum_i C_i \cdot \xi_i \quad (8)$$

where C_i represents organic compounds in all phases (Table 1s). As reported by Zhao et al. (2015), the average total IVOC to POA ratio is 20.4. This ratio was used to estimate the total concentration of organic compounds in both gas and particle phases. The mass fraction of organic compound *i* was taken from Zhao et al. (2015). As shown in Fig. S1, the modeled POA fit very well with measured POA.

As the concentrations of POA in this study were 13.5–62.3 μg m^{-3}, about 10 times higher than those in Chirico et al. (2010). The high concentration of POA would facilitate gas-particle partition of organic vapors (Odum et al., 1996; Kamens et al., 2011; Ye et al., 2016). If we diluted the exhaust to make the OA concentration in this study similar to that in Chirico et al. (2010), we can estimate the average EF_{POA} for Changan, Foton and JAC were 0.50, 0.18 and 0.12 g kg-$fuel^{-1}$, respectively. The EF_{POA} for Foton and JAC were comparable to the highest emission factor of POA (0.147 g kg-$fuel^{-1}$) reported by Chirico et al. (2010). However, the EF_{POA} for Changan was still higher than that in Chirico et al. (2010). If we diluted the exhaust to make the OA concentration in this study similar to that in Gordon et al. (2014b), the EF_{POA} for Changan, Foton and JAC were 0.45, 0.16 and 0.11 g kg-$fuel^{-1}$, respectively. They were all much higher than the EF_{POA} for HDDV at idling condition (0.047 g kg-$fuel^{-1}$) reported by Gordon et al. (2014b). Therefore, dilution is not the main reason for higher EF_{POA} in this study than those in previous studies.

Recent studies demonstrated a strong association between cardiovascular mortality and particle number concentration (Breitner et al., 2011; Leitte et al., 2011). European Union has set a particle number emission limit of 6×10^{11} # km^{-1} for Euro 6 diesel vehicles in 2008 and implemented it in 2011 (EU commission regulation No 459/2012). The emission factors of total particle number concentration (EF_{TN}) were calculated and presented in Fig. 2. The highest $EF_{TN} = 4.0 \times 10^{15}$ particles kg-$fuel^{-1}$ was measured from Changan medium-duty truck. The averaged EF_{TN} for Foton medium-duty passenger car and JAC heavy-duty truck were 7.6×10^{14} and 6.5×10^{14} particles kg-$fuel^{-1}$, respectively. The EF_{TN} obtained in this study were comparable with that of 0.3–21 $\times 10^{14}$ particles kg-$fuel^{-1}$ reported by Pirjola et al. (2016). By using 7.5 L/100 km (*i*CET, 2014) as the average diesel efficiency, and assuming a diesel oil density of 0.85 g mL^{-1} (Zhang et al., 2016), we could obtain mileage-based emission factors of particles for Changan, Foton and JAC as 2.6×10^{14}, 4.8×10^{13} and 4.2×10^{13} particles km^{-1}, respectively; they were all far beyond the EU limit. It is worth noting that the EF_{TN} were measured under real-world condition in Pirjola et al. (2016), while the operation mode was idling in this study. Since the EF_{TN} for the on-road measurements was 7–40 folds higher compared to the depot measurements (Pirjola et al., 2016), the EF_{TN} could be even higher when measured under on-road condition than obtained at idling condition.

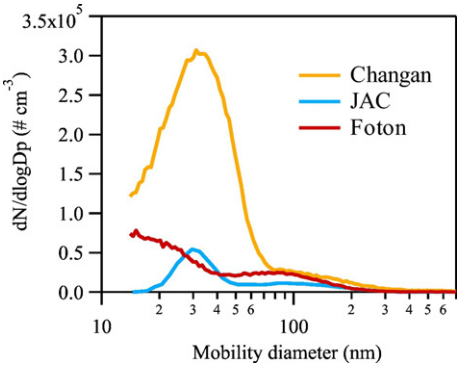

Fig. 3. Number size distributions of primarily emitted particles when the injection of exhaust was finished.

Fig. 3 showed the typical particle number size distributions for three types of vehicles. Consistent with previous studies (Rönkkö et al., 2007; Pirjola et al., 2016), a bimodal shape was observed with nucleation mode particles dominating the emissions of total particle number; the soot mode peaked at approximately 80 nm, while the nucleation mode distribution varied with different vehicles. It peaked at 30 nm for Changan and JAC and 20 nm for Foton. The distribution of nucleation mode particles in this study is different with that in previous studies with a peak at 10 nm (Rönkkö et al., 2007; Pirjola et al., 2016). Rönkkö et al. (2013) suggested that nucleation mode particles are formed by condensation of volatile compounds onto nonvolatile core, and the geometric mean diameter of the core particles increased as the fuel sulfur content (FSC) increased. Arnold et al. (2012) also found that the gaseous sulfuric acid (GSA) in the exhaust can promote the formation of nucleation particles, while the exhaust GSA was observed to decrease with the decrease of FSC. Since the sulfur content in China III diesel fuel is averaged 95.6 ppm in Guangzhou (Li et al., 2016), approximately 10 times higher than that in Rönkkö et al. (2007). It is worth noting that primary particle number concentrations from the three diesel vehicles correlated very well with BC concentrations measured by the Aethalometer, especially when they were diluted to very low concentrations (Fig. 4). So the particle number emission from diesel vehicles reflected their BC or soot emission.

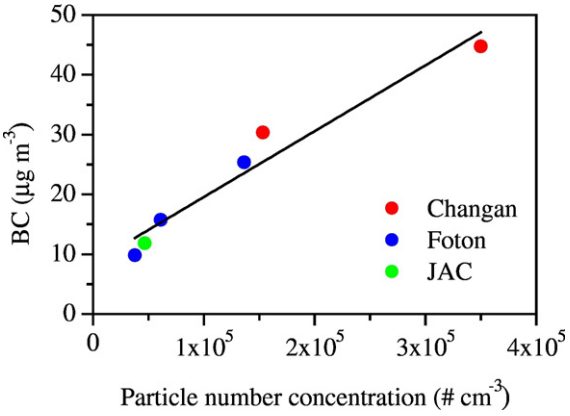

Fig. 4. Primary particle number concentrations measured by SMPS against that of BC measured by the Aethalometer.

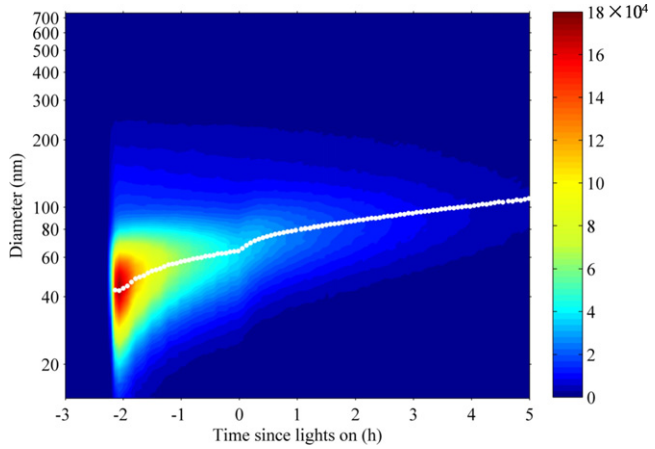

Fig. 5. Particle number size distributions as a function of time during a typical smog chamber experiment (Experiment 4). The white dots represent the evolution of median diameter during the experiment.

3.2. SOA formation from diesel vehicle exhausts

After turning on the lights, the wall-loss corrected OA started to climb with the formation of SOA (Fig. 1c). For example, the wall-loss corrected OA in Experiment 4 increased from 30.4 μg m^{-3} to 67.1 μg m^{-3} for ω = 0 case, and to 133.2 μg m^{-3} for ω = 1 case after 5 h photo-oxidation. Fig. 5 plotted the evolution of particle number distribution and median diameter during whole chamber experiment. Before the lights were turned on, the median diameter increased with a rate of 14.8 nm h^{-1}. As soon as the black lights were switched on, the particle growth rate was 21.0 nm h^{-1} in the first half hour, higher than that at dark condition, demonstrating the particle growth at illumination condition was not merely caused by particle wall loss or coagulation. As displayed in Fig. 5, there was no sign of increasing particle numbers with the increase of median diameters, meanwhile the mass concentration of OA measured by AMS increased from 21.7 to 26.9 μg m^{-3} within half an hour after the lights were switched on (Fig. 1c). This suggests particles grew by coating of the newly formed SOA on pre-existing particles, consistent with the results of Weitkamp et al. (2007).

As shown in Fig. 2, the PF_{SOA} ranged from 0.50 to 1.8 g kg-$fuel^{-1}$ for ω = 1 case. The EF_{SOA} obtained from this study were much higher than those reported in the literature, as the highest PF of SOA reported by Chirico et al. (2010) for a medium-duty diesel vehicle (MDDV) at idling condition in Switzerland is only 0.461 g kg-$fuel^{-1}$. The SOA/POA ratios for ω = 1 case in all the experiments were averaged 2.2 with a range from 0.7 to 3.4 in this study, lower than that of ~3 reported by Chirico et al. (2010) for a MDDV at idling condition with ω = 1, and ~10 reported by Gordon et al. (2014b) for a heavy-duty diesel vehicle (HDDV) at creep condition in the US. As the reaction condition including OH concentrations, temperature, relative humidity and VOC/NO_x ratios were similar to those in Chirico et al. (2010) and Gordon et al. (2014b), the lower SOA production might be due to difference in precursors. Zhao et al. (2015) found that IVOCs dominated the SOA formation from diesel exhaust. However, both this study and previous studies did not measure the concentrations of IVOCs. It's worth noting that the averaged O/C ratio of POA measured by AMS was 0.38 in this study, while it ranged 0.10–0.19 in Chirico et al. (2010). This indicates that POA investigated in this study was more oxidized than that in previous studies.

As reported by Liu et al. (2015a), the highest EF_{POA} and PF_{SOA} for gasoline vehicle exhaust in China are 0.0004 g kg-$fuel^{-1}$ and 0.044 g kg-$fuel^{-1}$, respectively, which are 1–3 orders of magnitude lower than those for diesel vehicle exhaust according to this study. As reported by Ou et al. (2010), the fuel consumption of diesel and gasoline for road transportation is 38.53 and 52.20 million tons in 2007, so the diesel derived OA would dominate overwhelmingly over the gasoline derived OA in the vehicle-related sector, despite a higher fraction of gasoline vehicles (83.5%) against that of diesel vehicles (15.2%) in China (MEPC, 2014). As the SOA/POA ratios ranged from 0.7 to 3.7, demonstrating controlling both POA and SOA are very important for diesel vehicles. Nevertheless, it is worth noting that the EF_{POA} and PF_{SOA} for diesel and gasoline vehicle exhausts were obtained under idling condition, the EF_{POA} and PF_{SOA} for on-road condition might be different.

3.3. SOA yield from traditional precursor VOCs

SOA production from a larger spectrum of C_2–C_{12} NMHCs measured offline other than that by PTR-ToF-MS was estimated using the following formula:

$$SOA_{predicted} = \sum_i \Delta X_i \times Y_i \quad (9)$$

where $SOA_{predicted}$ (μg m^{-3}) is the predicted SOA concentration from precursor *i*; ΔX_i (μg m^{-3}) is the mass of the reacted precursor *i*; and Y_i (%) is the SOA yield of precursor *i*. In this study, SOA yields for benzene, toluene, and m-xylene were estimated using the two-product model curves taken from Ng et al. (2007), whilst those for C_3-benzene and C_4-benzene are taken from Odum et al. (1997). SOA yields for alkanes and alkenes were estimated with the method of Tsimpidi et al. (2010). Briefly, alkanes and alkenes were divided into 9 groups. The SOA yields for each group were estimated through the volatility basis-set approach.

As presented in Table 3, the predicted SOA concentrations from 65 NMHCs accounted for less than 3% of the observed SOA production. Similarly, Weitkamp et al. (2007) reported that SOA formed from 58 known precursors, including aromatics, alkanes and alkenes, explained less than 8% of the new particle mass in diesel exhaust simulation. It demonstrated that traditional VOC precursors could not explain the amount of diesel SOA formation. One possible reason is that the yields of aromatic hydrocarbons in complex mixtures might be higher than those under

Table 3
The predicted SOA production from each aromatics, alkanes and alkenes in all experiments.

Expt. no.	Predicted SOA (μg m^{-3})							Predicted SOA/measured SOA[a]
	Benzene	Toluene	C_2-benzene	C_3-benzene	C_4-benzene	Alkanes	Alkenes	
1	0.015	0.019	0.022	0.081	0.085	0.022	0.080	2.6%
2	0.202	0.028	0.050	0.068	0.114	0.002	0.012	2.2%
3	0.069	0.013	0.051	0.054	0.068	0.038	0.082	1.4%
4	0.127	0.055	0.013	0.007	0.017	0.028	0.013	0.8%
5	0.074	0.012	0.082	0.075	0.108	0.030	0.229	1.6%
6	0.237	0.213	0.496	0.018	0.007	0.029	0.090	3.1%
7	0.164	0.065	0.014	0.052	0.077	0.049	0.019	1.2%
8	0.329	0.072	0.067	0.124	0.229	0.052	0.34	2.3%

[a] Measured SOA were wall loss corrected at ω = 0.

single precursor conditions (Song et al., 2007), resulting in the SOA mass being underestimated. However, even if we took a higher aromatics yield, such as the effective SOA yield of ~30% reported by Gordon et al. (2014b), aromatics still only account for less than 10% of the total SOA. The unexplained part is probably from the photo-oxidation of IVOCs (Weitkamp et al., 2007; Robinson et al., 2007). Zhao et al. (2015) reported that IVOCs dominated the SOA formation from diesel exhaust. However, over 90% of the IVOCs were not speciated (Zhao et al., 2015). Therefore, the SOA formation from IVOCs deserves further investigation.

4. Conclusions

In this study, primary emission of particulate matters from three types of diesel vehicles widely used in China and SOA formation from the exhaust under photo-oxidation were investigated. The EF_{BC} and EF_{TN} were 0.15–0.51 g kg-fuel^{-1} and 0.65–4.0 × 10^{15} # kg-fuel^{-1}, respectively. The primary number concentrations demonstrated well correlation with the BC concentrations. Measured EF_{POA} and PF_{SOA} were 0.19 and 0.61 g kg-fuel^{-1} for JAC, 0.18–0.34 and 0.56–0.76 g kg-fuel^{-1} for Foton, 0.72–0.91 and 0.50–1.8 g kg-fuel^{-1} for Changan, respectively, which are all higher than those previously reported in similar studies in Europe and the US. These EF_{POA} and PF_{SOA} values were also 1–3 orders of magnitude higher than those for gasoline vehicle exhaust. Therefore, although the diesel vehicle population is much less than that of gasoline in China, it still plays a vital role in the contribution of primary and secondary OA. According to our study, less than 3% of diesel SOA production can be explained by traditional SOA precursors, consistent with previous diesel exhaust studies. This demonstrates that the role of other precursors, including IVOCs, deserves further investigation both in the scientific and regulatory communities for diesel vehicle emission control. It should be noted that at present all the experiments for SOA formation from both gasoline and diesel vehicles in China were conducted under idling condition. The emission of POA as well as formation of SOA under different operating modes, especially on-road conditions, needs further investigation.

Acknowledgments

This study was supported by the Strategic Priority Research Program of the Chinese Academy of Sciences (XDB05010200), National Key Research and Development Program (2016YFC0202204) and the National Natural Science Foundation of China (41571130031/41530641).

Appendix A. Supplementary data

Supplementary data to this article can be found online at http://dx.doi.org/10.1016/j.scitotenv.2017.03.088.

References

Abdul-Khalek, I., Kittelson, D., Brear, F., 1999. The influence of dilution conditions on diesel exhaust particle size distribution measurements. SAE Tech. Pap. Ser., No. 1999-01-1142.

Arnold, F., Pirjola, L., Rönkkö, T., Reichl, U., Schlager, H., Lähde, T., Heikkilä, J., Keskinen, J., 2012. First online measurements of sulfuric acid gas in modern heavy-duty diesel engine exhaust: implications for nanoparticle formation. Environ. Sci. Technol. 46, 11227–11234.

Atkinson, R., Arey, J., 2003. Atmospheric degradation of volatile organic compounds. Chem. Rev. 103, 4605–4638.

Barmet, P., Dommen, J., DeCarlo, P.F., Tritscher, T., Praplan, A.P., Platt, S.M., Prevot, A.S.H., Donahue, N.M., Baltensperger, U., 2012. OH clock determination by proton transfer reaction mass spectrometry at an environmental chamber. Atmos. Meas. Tech. 5, 647–656.

Breitner, S., Liu, L.Q., Cyrys, J., Bruske, I., Franck, U., Schlink, U., Leitte, A.M., Herbarth, O., Wiedensohler, A., Wehner, B., Hu, M., Pan, X.C., Wichmann, H.E., Peters, A., 2011. Sub-micrometer particulate air pollution and cardiovascular mortality in Beijing, China. Sci. Total Environ. 409, 5196–5204.

Brook, R.D., Rajagopalan, S., Pope 3rd, C.A., Brook, J.R., Bhatnagar, A., Diez-Roux, A.V., Holguin, F., Hong, Y., Luepker, R.V., Mittleman, M.A., Peters, A., Siscovick, D., Smith Jr., S.C., Whitsel, L., Kaufman, J.D., American Heart Association Council on, E., Prevention, C.o.t.K.i.C.D., Council on Nutrition, P.A., Metabolism, 2010. Particulate matter air pollution and cardiovascular disease: an update to the scientific statement from the American Heart Association. Circulation 121, 2331–2378.

Chen, Y., Zheng, M., Edgerton, E.S., Ke, L., Sheng, G., Fu, J., 2012. $PM_{2.5}$source apportionment in the southeastern U.S.: spatial and seasonal variations during 2001–2005. J. Geophys. Res. 117, D08304.

China Association of Automobile Manufacturers (CAAM), 2011. China Automotive Industry Yearbook. 2011.

Chirico, R., DeCarlo, P.F., Heringa, M.F., Tritscher, T., Richter, R., Prevot, A.S.H., Dommen, J., Weingartner, E., Wehrle, G., Gysel, M., Laborde, M., Baltensperger, U., 2010. Impact of aftertreatment devices on primary emissions and secondary organic aerosol formation potential from in-use diesel vehicles: results from smog chamber experiments. Atmos. Chem. Phys. 10, 11545–11563.

Cocker, D.R., Mader, B.T., Kalberer, M., Flagan, R.C., Seinfeld, J.H., 2001. The effect of water on gas-particle partitioning of secondary organic aerosol: II. m-Xylene and 1,3,5-trimethylbenzene photooxidation systems. Atmos. Environ. 35, 6073–6085.

Cross, E.S., Sappok, A.G., Wong, V.W., Kroll, J.H., 2015. Load-dependent emission factors and chemical characteristics of IVOCs from a medium-duty diesel engine. Environ. Sci. Technol. 49, 13483–13491.

Cui, H., Chen, W., Dai, W., Liu, H., Wang, X., He, K., 2015. Source apportionment of $PM_{2.5}$ in Guangzhou combining observation data analysis and chemical transport model simulation. Atmos. Environ. 116, 262–271.

DeCarlo, P.F., Kimmel, J.R., Trimborn, A., Northway, M.J., Jayne, J.T., Aiken, A.C., Gonin, M., Fuhrer, K., Horvath, T., Docherty, K.S., Worsnop, D.R., Jimenez, J.L., 2006. Field-deployable, high-resolution, time-of-flight aerosol mass spectrometer. Anal. Chem. 78, 8281–8289.

Donahue, N.M., Robinson, A.L., Stanier, C.O., Pandis, S.N., 2006. Coupled partitioning, dilution, and chemical aging of semivolatile organics. Environ. Sci. Technol. 40, 2635–2643.

Dunmore, R.E., Hopkins, J.R., Lidster, R.T., Lee, J.D., Evans, M.J., Rickard, A.R., Lewis, A.C., Hamilton, J.F., 2015. Diesel-related hydrocarbons can dominate gas phase reactive carbon in megacities. Atmos. Chem. Phys. 15, 9983–9996.

EU Commission Regulation No 459/2012. Commission Regulation (EU) No 459/2012 of 29 May 2012, 2012. Amending regulation (EC) no 715/2007 of the European Parliament and of the Council and commission regulation (EC) no 692/2008 as regards emissions from light passenger and commercial vehicles (Euro 6). Off. J. Eur. Union L 142, 16–24.

Gordon, T.D., Presto, A.A., May, A.A., Nguyen, N.T., Lipsky, E.M., Donahue, N.M., Gutierrez, A., Zhang, M., Maddox, C., Rieger, P., Chattopadhyay, S., Maldonado, H., Maricq, M.M., Robinson, A.L., 2014a. Secondary organic aerosol formation exceeds primary particulate matter emissions for light-duty gasoline vehicles. Atmos. Chem. Phys. 14, 4661–4678.

Gordon, T.D., Presto, A.A., Nguyen, N.T., Robertson, W.H., Na, K., Sahay, K.N., Zhang, M., Maddox, C., Rieger, P., Chattopadhyay, S., Maldonado, H., Maricq, M.M., Robinson, A.L., 2014b. Secondary organic aerosol production from diesel vehicle exhaust: impact of aftertreatment, fuel chemistry and driving cycle. Atmos. Chem. Phys. 14, 4643–4659.

Guangzhou Environmental Protection Bureau, 2015. Report on the State of the Environment in Guangzhou.

Guo, S., Hu, M., Zamora, M.L., Peng, J., Shang, D., Zheng, J., Du, Z., Wu, Z., Shao, M., Zeng, L., Molina, M.J., Zhang, R., 2014. Elucidating severe urban haze formation in China. Proc. Natl. Acad. Sci. U. S. A. 111, 17373–17378.

Guo, H., Ling, Z.H., Cheung, K., Jiang, F., Wang, D.W., Simpson, I.J., Barletta, B., Meinardi, S., Wang, T.J., Wang, X.M., Saunders, S.M., Blake, D.R., 2013. Characterization of photochemical pollution at different elevations in mountainous areas in Hong Kong. Atmos. Chem. Phys. 13, 3881–3898.

Huang, X.F., Yu, J.Z., He, L.Y., Hu, M., 2006. Size distribution characteristics of elemental carbon emitted from Chinese vehicles: results of a tunnel study and atmospheric implications. Environ. Sci. Technol. 40, 5355–5360.

Huang, R.J., Zhang, Y., Bozzetti, C., Ho, K.F., Cao, J.J., Han, Y., Daellenbach, K.R., Slowik, J.G., Platt, S.M., Canonaco, F., Zotter, P., Wolf, R., Pieber, S.M., Bruns, E.A., Crippa, M., Ciarelli, G., Piazzalunga, A., Schwikowski, M., Abbaszade, G., Schnelle-Kreis, J., Zimmermann, R., An, Z., Szidat, S., Baltensperger, U., El Haddad, I., Prevot, A.S., 2014. High secondary aerosol contribution to particulate pollution during haze events in China. Nature 514, 218–222.

Huo, H., Zhang, Q., He, K., Yao, Z., Wang, X., Zheng, B., Streets, D.G., Wang, Q., Ding, Y., 2011. Modeling vehicle emissions in different types of Chinese cities: importance of vehicle fleet and local features. Environ. Pollut. 159, 2954–2960.

Innovation Center for Energy and Transportation (iCET), 2014. China Passenger Vehicle Fuel Consumption Development Annual Report 2014. http://icet.org.cn/admin/upload/20141018123825 77.pdf.

Jayne, J.T., Leard, D.C., Zhang, X., Davidovits, P., Smith, K.A., Kolb, C.E., Worsnop, D.R., 2000. Development of an aerosol mass spectrometer for size and composition analysis of submicron particles. Aerosol Sci. Technol. 33, 49–70.

Jordan, A., Haidacher, S., Hanel, G., Hartungen, E., Märk, L., Seehauser, H., Schottkowsky, R., Sulzer, P., Märk, T.D., 2009. A high resolution and high sensitivity proton-transfer-reaction time-of-flight mass spectrometer (PTR-ToF-MS). Int. J. Mass Spectrom. 286, 122–128.

Kamens, R.M., Zhang, H., Chen, E.H., Zhou, Y., Parikh, H.M., Wilson, R.L., Galloway, K.E., Rosen, E.P., 2011. Secondary organic aerosol formation from toluene in an atmospheric hydrocarbon mixture: water and particle seed effects. Atmos. Environ. 45, 2324–2334.

Kirchstetter, T.W., Novakov, T., 2007. Controlled generation of black carbon particles from a diffusion flame and applications in evaluating black carbon measurement methods. Atmos. Environ. 41, 1874–1888.

Lange, W.W., Schäfer, A., Le'Jeune, A., Naber, D., Reglitzky, A.A., Gairing, M., 1993. The influence of fuel properties on exhaust emissions from advanced mercedes benz diesel engines. SAE Tech. Pap. Ser., No. 932685.
Leitte, A.M., Schlink, U., Herbarth, O., Wiedensohler, A., Pan, X.C., Hu, M., Richter, M., Wehner, B., Tuch, T., Wu, Z.J., Yang, M.J., Liu, L.Q., Breitner, S., Cyrys, J., Peters, A., Wichmann, H.E., Franck, U., 2011. Size-segregated particle number concentrations and respiratory emergency room visits in Beijing, China. Environ. Health Perspect. 119, 508–513.
Lelieveld, J., Evans, J.S., Fnais, M., Giannadaki, D., Pozzer, A., 2015. The contribution of outdoor air pollution sources to premature mortality on a global scale. Nature 525, 367–371.
Li, G., Zhang, Y., Fu, X., Li, Z., Huang, Z., Wang, X., 2016. Sulfur contents in commercial available gasoline and diesel oils sold in 8 Chinese cities. China J. Environ. Sci. Technol. 39, 384–388 (in Chinese).
Lindinger, W., Hansel, A., Jordan, A., 1998. On-line monitoring of volatile organic compounds at pptv levels by means of proton-transfer-reaction mass spectrometry (PTR-MS) medical applications, food control and environmental research. Int. J. Mass Spectrom. Ion Process. 173, 191–241.
Lipsky, E.M., Robinson, A.L., 2006. Effects of dilution on fine particle mass and partitioning of semivolatile organics in diesel exhaust and wood smoke. Environ. Sci. Technol. 40, 155–162.
Liu, Z., Guan, D., Wei, W., Davis, S.J., Ciais, P., Bai, J., Peng, S., Zhang, Q., Hubacek, K., Marland, G., Andres, R.J., Crawford-Brown, D., Lin, J., Zhao, H., Hong, C., Boden, T.A., Feng, K., Peters, G.P., Xi, F., Liu, J., Li, Y., Zhao, Y., Zeng, N., He, K., 2015b. Reduced carbon emission estimates from fossil fuel combustion and cement production in China. Nature 524, 335–338.
Liu, H., He, K., Lents, J.M., Wang, Q., Tolvett, S., 2009. Characteristics of diesel truck emission in China based on portable emissions measurement systems. Environ. Sci. Technol. 43, 9507–9511.
Liu, T., Wang, X., Deng, W., Hu, Q., Ding, X., Zhang, Y., He, Q., Zhang, Z., Lü, S., Bi, X., Chen, J., Yu, J., 2015a. Secondary organic aerosol formation from photochemical aging of light-duty gasoline vehicle exhausts in a smog chamber. Atmos. Chem. Phys. 15, 9049–9062.
Liu, T., Wang, X., Wang, B., Ding, X., Deng, W., Lu, S., Zhang, Y., 2014. Emission factor of ammonia (NH_3) from on-road vehicles in China: tunnel tests in urban Guangzhou. Environ. Res. Lett. 9, 064027.
Mi, H.H., Lee, W.J., Chen, C.B., Yang, H.H., Wu, S.J., 2000. Effect of fuel aromatic content on PAH emission from a heavy-duty diesel engine. Chemosphere 41, 1783–1790.
Ministry of Environmental Protection of China (MEPC), 2014. China Vehicle Emission Control Annual Report.
Miracolo, M.A., Drozd, G.T., Jathar, S.H., Presto, A.A., Lipsky, E.M., Corporan, E., Robinson, A.L., 2012. Fuel composition and secondary organic aerosol formation: gas-turbine exhaust and alternative aviation fuels. Environ. Sci. Technol. 46, 8493–8501.
Nakao, S., Shrivastava, M., Nguyen, A., Jung, H., Cocker, D., 2011. Interpretation of secondary organic aerosol formation from diesel exhaust photooxidation in an environmental chamber. Aerosol Sci. Technol. 45, 964–972.
Ng, N.L., Kroll, J.H., Chan, A.W.H., Chhabra, P.S., Flagan, R.C., Seinfeld, J.H., 2007. Secondary organic aerosol formation from m-xylene, toluene, and benzene. Atmos. Chem. Phys. 7, 3909–3922.
Odum, J.R., Hoffmann, T., Bowman, F., Collins, D., Flagan, R.C., Seinfeld, J.H., 1996. Gas/particle partitioning and secondary organic aerosol yields. Environ. Sci. Technol. 30, 2580–2585.
Odum, J.R., Jungkamp, T.P.W., Griffin, R.J., Flagan, R.C., Seinfeld, J.H., 1997. The atmospheric aerosol-forming potential of whole gasoline vapor. Science 276, 96–99.
Ots, R., Young, D.E., Vieno, M., Xu, L., Dunmore, R.E., Allan, J.D., Coe, H., Williams, L.R., Herndon, S.C., Ng, N.L., Hamilton, J.F., Bergström, R., Di Marco, C., Nemitz, E., Mackenzie, I.A., Kuenen, J.J.P., Green, D.C., Reis, S., Heal, M.R., 2016. Simulating secondary organic aerosol from missing diesel-related intermediate-volatility organic compound emissions during the Clean Air for London (ClearfLo) campaign. Atmos. Chem. Phys. 16, 6453–6473.
Ou, X., Zhang, X., Chang, S., 2010. Scenario analysis on alternative fuel/vehicle for China's future road transport: life-cycle energy demand and GHG emissions. Energy Policy 38, 3943–3956.
Pirjola, L., Dittrich, A., Niemi, J.V., Saarikoski, S., Timonen, H., Kuuluvainen, H., Järvinen, A., Kousa, A., Rönkkö, T., Hillamo, R., 2016. Physical and chemical characterization of real-world particle number and mass emissions from city buses in Finland. Environ. Sci. Technol. 50, 294–304.
Pope, C.A., Ezzati, M., Dockery, D.W., 2009. Fine-particulate air pollution and life expectancy in the United States. N. Engl. J. Med. 360, 376–386.
Presto, A.A., Gordon, T.D., Robinson, A.L., 2014. Primary to secondary organic aerosol: evolution of organic emissions from mobile combustion sources. Atmos. Chem. Phys. 14, 5015–5036.
Reff, A., Bhave, P.V., Simon, H., Pace, T.G., Pouliot, G.A., Mobley, J.D., Houyoux, M., 2009. Emissions inventory of $PM_{2.5}$ trace elements across the United States. Environ. Sci. Technol. 43, 5790–5796.
Robinson, A.L., Donahue, N.M., Shrivastava, M.K., Weitkamp, E.A., Sage, A.M., Grieshop, A.P., Lane, T.E., Pierce, J.R., Pandis, S.N., 2007. Rethinking organic aerosols: semivolatile emissions and photochemical aging. Science 315, 1259–1262.
Rogge, W.F., Hildemann, L.M., Mazurek, M.A., Cass, G.R., Simoneit, B.R.T., 1993. Sources of fine organic aerosol. 2. Noncatalyst and catalyst-equipped automobiles and heavy-duty diesel trucks. Environ. Sci. Technol. 27, 636–651.
Rönkkö, T., Lähde, T., Heikkilä, J., Pirjola, L., Bauschke, U., Arnold, F., Schlager, H., Rothe, D., Yli-Ojanperä, J., Keskinen, J., 2013. Effects of gaseous sulphuric acid on diesel exhaust nanoparticle formation and characteristics. Environ. Sci. Technol. 47, 11882–11889.
Rönkkö, T., Virtanen, A., Kannosto, J., Keskinen, J., Lappi, M., Pirjola, L., 2007. Nucleation mode particles with a nonvolatile core in the exhaust of a heavy duty diesel vehicle. Environ. Sci. Technol. 41, 6384–6389.
Samy, S., Zielinska, B., 2010. Secondary organic aerosol production from modern diesel engine emissions. Atmos. Chem. Phys. 10, 609–625.
Schnaiter, M., Linke, C., Möhler, O., Naumann, K.H., Saathoff, H., Wagner, R., Schurath, U., Wehner, B., 2005. Absorption amplification of black carbon internally mixed with secondary organic aerosol. J. Geophys. Res. 110, D19204.
Shiraiwa, M., Kondo, Y., Iwamoto, T., Kita, K., 2010. Amplification of light absorption of black carbon by organic coating. Aerosol Sci. Technol. 44, 46–54.
Shrivastava, M.K., Lipsky, E.M., Stanier, C.O., Robinson, A.L., 2006. Modeling semivolatile organic aerosol mass emissions from combustion systems. Environ. Sci. Technol. 40, 2671–2677.
Song, C., Na, K., Warren, B., Malloy, Q., Cocker III, D.R., 2007. Impact of propene on secondary organic aerosol formation from m-xylene. Environ. Sci. Technol. 41, 6990–6995.
Stone, E.A., Snyder, D.C., Sheesley, R.J., Sullivan, A.P., Weber, R.J., Schauer, J.J., 2008. Source apportionment of fine organic aerosol in Mexico City during the MILAGRO experiment 2006. Atmos. Chem. Phys. 8, 1249–1259.
Tsimpidi, A.P., Karydis, V.A., Zavala, M., Lei, W., Molina, L., Ulbrich, I.M., Jimenez, J.L., Pandis, S.N., 2010. Evaluation of the volatility basis-set approach for the simulation of organic aerosol formation in the Mexico City metropolitan area. Atmos. Chem. Phys. 10, 525–546.
Wang, H., Fu, L., Zhou, Y., Du, X., Ge, W., 2010. Trends in vehicular emissions in China's mega cities from 1995 to 2005. Environ. Pollut. 158, 394–400.
Wang, X., Liu, T., Bernard, F., Ding, X., Wen, S., Zhang, Y., Zhang, Z., He, Q., Lu, S., Chen, J., Saunders, S., Yu, J., 2014. Design and characterization of a smog chamber for studying gas-phase chemical mechanisms and aerosol formation. Atmos. Meas. Tech. 7, 301–313.
Wang, X., Tian, Z., Zhang, Y., 2015. Influence of fuel quality on vehicle emission and economic analysis of upgrading fuel quality in China. Bull. Chin. Acad. Sci. 30, 535–541 (in Chinese).
Weitkamp, E.A., Sage, A.M., Pierce, J.R., Donahue, N.M., Robinson, A.L., 2007. Organic aerosol formation from photochemical oxidation of diesel exhaust in a smog chamber. Environ. Sci. Technol. 41, 6969–6975.
Wu, B., Shen, X., Cao, X., Yao, Z., Wu, Y., 2016. Characterization of the chemical composition of $PM_{2.5}$ emitted from on-road China III and China IV diesel trucks in Beijing, China. Sci. Total Environ. 551–552, 579–589.
Wu, B., Shen, X., Cao, X., Zhang, W., Wu, H., Yao, Z., 2015. Carbonaceous composition of $PM_{2.5}$ emitted from on-road China III diesel trucks in Beijing, China. Atmos. Environ. 116, 216–224.
Wu, Y., Wang, R., Zhou, Y., Lin, B., Fu, L., He, K., Hao, J., 2010. On-road vehicle emission control in Beijing: past, present, and future. Environ. Sci. Technol. 45, 147–153.
Xu, H., Wang, X., Pöschl, U., Feng, S., Wu, D., Yang, L., Li, S., Song, W., Sheng, G., Fu, J., 2008. Genotoxicity of total and fractionated extractable organic matter in fine air particulate matter from urban Guangzhou: comparison between haze and nonhaze episodes. Environ. Toxicol. Chem. 27, 206–212.
Yanowitz, J., McCormick, R.L., Graboski, M.S., 2000. In-use emissions from heavy-duty diesel vehicles. Environ. Sci. Technol. 34, 729–740.
Yao, Z., Shen, X., Ye, Y., Cao, X., Jiang, X., Zhang, Y., He, K., 2015. On-road emission characteristics of VOCs from diesel trucks in Beijing, China. Atmos. Environ. 103, 87–93.
Ye, P.L., Ding, X., Hakala, J., Hofbauer, V., Robinson, E.S., Donahue, N.M., 2016. Vapor wall loss of semi-volatile organic compounds in a Teflon chamber. Aerosol Sci. Technol. 50, 822–834.
Yi, Z., Wang, X., Sheng, G., Zhang, D., Zhou, G., Fu, J., 2007. Soil uptake of carbonyl sulfide in subtropical forests with different successional stages in south China. J. Geophys. Res. 112, D08302.
Yue, X., Wu, Y., Hao, J., Pang, Y., Ma, Y., Li, Y., Li, B., Bao, X., 2015. Fuel quality management versus vehicle emission control in China, status quo and future perspectives. Energy Policy 79, 87–98.
Zhang, Q., Streets, D.G., Carmichael, G.R., He, K.B., Huo, H., Kannari, A., Klimont, Z., Park, I.S., Reddy, S., Fu, J.S., Chen, D., Duan, L., Lei, Y., Wang, L.T., Yao, Z.L., 2009. Asian emissions in 2006 for the NASA INTEX-B mission. Atmos. Chem. Phys. 9, 5131–5153.
Zhang, Y., Wang, X., Blake, D.R., Li, L., Zhang, Z., Wang, S., Guo, H., Lee, F.S.C., Gao, B., Chan, L., Wu, D., Rowland, F.S., 2012. Aromatic hydrocarbons as ozone precursors before and after outbreak of the 2008 financial crisis in the Pearl River Delta region, south China. J. Geophys. Res. 117, D15306.
Zhang, Y., Wang, X., Li, G., Yang, W., Huang, Z., Zhang, Z., Huang, X., Deng, W., Liu, T., Huang, Z., Zhang, Z., 2015. Emission factors of fine particles, carbonaceous aerosols and traces gases from road vehicles: Recent tests in an urban tunnel in the Pearl River Delta, China. Atmos. Environ. 122, 876–884.
Zhang, Y., Wang, X., Wen, S., Herrmann, H., Yang, W., Huang, X., Zhang, Z., Huang, Z., He, Q., George, C., 2016. On-road vehicle emissions of glyoxal and methylglyoxal from tunnel tests in urban Guangzhou, China. Atmos. Environ. 127, 55–60.
Zhao, Y., Nguyen, N.T., Presto, A.A., Hennigan, C.J., May, A.A., Robinson, A.L., 2015. Intermediate volatility organic compound emissions from on-road diesel vehicles: chemical composition, emission factors, and estimated secondary organic aerosol production. Environ. Sci. Technol. 49, 11516–11526.
Zhao, L., Wang, X., He, Q., Wang, H., Sheng, G., Chan, L.Y., Fu, J., Blake, D.R., 2004. Exposure to hazardous volatile organic compounds, PM_{10} and CO while walking along streets in urban Guangzhou, China. Atmos. Environ. 38, 6177–6184.
Zheng, X., Wu, Y., Jiang, J., Zhang, S., Liu, H., Song, S., Li, Z., Fan, X., Fu, L., Hao, J., 2015. Characteristics of on-road diesel vehicles: black carbon emissions in Chinese cities based on portable emissions measurement. Environ. Sci. Technol. 49, 13492–13500.